Langmuir

ARTICLE

pubs.acs.org/Langmuir

Tuning Surface Wettability of $In_xGa_{(1-x)}N$ Nanotip Arrays by Phosphonic Acid Modification and Photoillumination

Ruigong Su,[†,‡,§] Haibin Liu,[†] Tao Kong,[†] Qin Song,[†] Ning Li,[†,‡,§] Gang Jin,[§] and Guosheng Cheng*[,†,‡]

[†]Suzhou Institute of Nano-Tech and Nano-Bionics, Chinese Academy of Sciences, 398 Ruoshui Road, Suzhou Industrial Park, Jiangsu 215123, People's Republic of China

[‡]Graduate University of the Chinese Academy of Sciences, Beijing 100049, People's Republic of China

[§]Institute of Mechanics, Chinese Academy of Sciences, Beijing 100190, People's Republic of China

Supporting Information

ABSTRACT: We report a facile route to reversibly tune surface wettability of $In_xGa_{(1-x)}N$ (InGaN) nanotip arrays by octylphosphonic acid (OPA) modification and ultraviolet−visible (UV−vis) light illuminations. Well-aligned InGaN nanotip arrays were grown by chemical vapor deposition (CVD). OPA was covalently attached to the InGaN nanotip surface, which was initially oxidized in Piranha solution. Because of the high surface energy of polar groups, OPA-coated InGaN nanotip arrays demonstrated superhydrophobic properties (contact angle of 154°). Transitions between superhydrophobicity and hydrophilicity were obtained through OPA adsorption and UV−vis light illumination. The InGaN nanotip surface chemistry was further characterized by X-ray photoelectron spectroscopy (XPS), which suggested a scission mechanism at P−C and MO−P (M = In and Ga) bonds of bound OPA molecules. Meanwhile, no significant surface degradation was observed after the OPA modification and phototreatments.

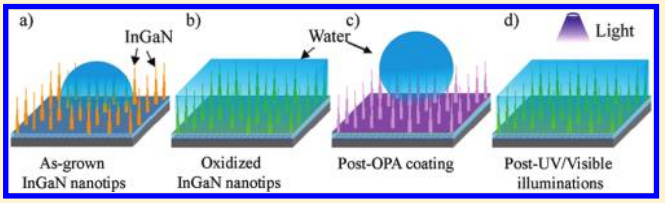

INTRODUCTION

Surface properties of materials attract more and more attention because of their essence of catalysis chemistry and semiconductor electronic devices.[1] Among them, tremendous efforts have been made on wetting behaviors of nanostructures because of the high ratio of the liquid−air contact area to apparent surface area,[2] such as Si,[3] TiO_2 nanobelts,[4] ZnO nanowires, and WO_x nanowires.[5] The wetting properties of these nanomaterials can be adjusted via topological sturctures,[6] surface chemical modifications,[7] heat, light,[8] and electric fields.[3a,9]

Under light illumination, the nature of surface chemistry and electronic structures of the photosensitive materials can be modified, resulting in transformation of polarity, reflective index, and electronic and magnetic properties. On the basis of these changes, commercial self-cleaning glass, antifogging materials, manipulation of small volume liquids, and even new printing technologies have been developed.[10] Because of the high surface/volume and liquid−air to liquid−solid ratio, novel nanomaterials with enhanced photodecomposition and superhydrophobic and superhydrophilic properties have been intensively studied. Kwak et al.[11] modified ZnO nanowire arrays by fatty acids with different lengths to obtain a patterned superhydrophobic−superhydrophilic surface via ultraviolet (UV) illumination. Meanwhile, TiO_2 with a band gap of 3.2 eV, which can adsorb lights with wavelengths less than 387 nm, is considered to be one of the most promising metal oxides in self-cleaning products. Because TiO_2 adsorbs UV light to generate electron−hole pairs, which produce active radicals (e.g., •OH and $•O_2^-$)[12] in aqueous solutions, it can be widely used in fields of photocatalysis and surface modifications. However, in comparison to UV, visible light dominates the majority of a solar spectrum. The wetting behavior of the surface of a material under visible illumination is greatly appreciated for metal protection and self-cleaning applications at an ambient condition. Nonetheless, owing to synthesis limitations, it is still a challenge to develop wide-band-gap semiconductors to harvest visible light to tune the surface wettability. For example, Wang et al.[13] attempted to dope TiO_2 with nitrogen at low temperatures to investigate visible-light-driven switchable hydrophobic to hydrophilic properties. Although progress has been made, doping stabilities and efficiencies are still critical issues. Thus, novel nanomaterials with tunable band gaps over the whole solar spectrum are highly demanded.

Recently, with a wide tunable band gap, high electron mobility,[14] and high stability in aqueous solution, Group III−V materials have been considered as excellent candidates for photocatalysis,[15] bioelectronics,[16] and water splitting for hydrogen gas.[17] $In_xGa_{(1-x)}N$ (InGaN) is a well-known material with a band gap ranging from 0.7 to 3.4 eV, depending upon the indium concentration percentage.[18] It was reported that hydrogen generation was performed via InGaN-based solar water splitting, covering an entire solar spectrum.[17b,19] Furthermore, InGaN demonstrates no significant degradation in aqueous solutions

Received: April 18, 2011
Revised: September 23, 2011
Published: September 27, 2011

Scheme 1. Schematic Diagrams of Surface Wettability Transitions of InGaN Nanotip Arrays after (a) CVD Synthesis, (b) Piranha Solution Oxidation, (c) OPA Modification, and (d) Light Illumination

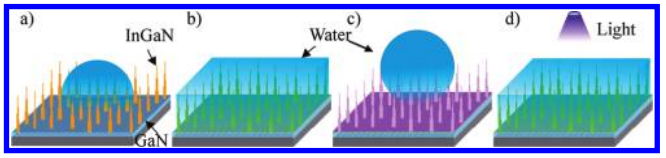

because of their small lattice constants and the strong bonding energy of In−N and Ga−N.[19b,20] Despite the remarkable achievements of InGaN by metal−organic chemical vapor deposition synthesis and spectacular optoelectronic applications,[21,22] less effort has been made on their wetting behaviors. In this paper, we report an efficient approach to tune the surface wettability of InGaN using phosphonic acid modification and photoillumination. The influence of UV and visible light on the surface wettability has been quantified.

EXPERIMENTAL SECTION

Schematic Diagrams of Wettability Measurements. The proposed method was schematically illustrated in Scheme 1. First, well-aligned InGaN nanotip arrays showing hydrophobic property (Scheme 1a) were grown on a GaN substrate on a silicon wafer. After immersion in Piranha solution for 30 min, an outer layer of the InGaN nanotip was oxidized to In_2O_3, Ga_2O_3, or both, resulting in hydrophilic property (Scheme 1b). Octylphosphonic acid (OPA) was then covalently attached to the InGaN nanotip surfaces, demonstrating once again a hydrophobic property (Scheme 1c). Under the illuminations of UV or visible lights, bonds between P−C and MO−P in OPA are subjected to be broken, rendering a hydrophilic surface (Scheme 1d).

Synthesis of InGaN Nanotip Arrays. InGaN nanotip arrays were synthesized using $InCl_3$, $GaCl_3$, and NH_3 [flow rate at 393 standard cubic centimeters (sccm)] and Ar (70 sccm) as In, Ga, and N sources and carrier gas, respectively. A synthetic reaction took place in a 2 in. diameter quartz tube, which was housed in a homemade programmable chemical vapor deposition (CVD) system. A Si (001) wafer was used as a substrate. $InCl_3$ and $GaCl_3$ were placed at different sites in a quartz tube. A synthesis route for InGaN nanotip arrays was briefly presented. Initially, the CVD system was heated to 700 °C and maintained until the end of the reaction. $GaCl_3$ precursors were then heated to 75 °C and kept for 1 h to grow GaN film on the substrate. Finally, the $GaCl_3$ precursors were cooled to 40 °C, while the $InCl_3$ precursors were heated to 350 °C and kept for 1 h. After the preceding reaction steps, InGaN nanotip arrays were obtained on the GaN surface on the silicon wafer.

Surface Modification by OPA and Ultraviolet−Visible (UV−vis) Light-Induced Wettability Measurements. InGaN nanotip surfaces were chemically modified by immersing the samples in a 5 mM OPA aqueous solution for 24 h at room temperature, followed by intense deionized (DI) water rinsing (Millipore system). The samples were then dried in a flow of N_2 stream. OPA-Modified InGaN substrates were placed in DI water under UV illuminations of a 400 W mercury lamp (UV) and visible illuminations of a 300 W xenon lamp (wavelength ranging from 200 to 1800 nm, with a 400 nm high-pass filter) at room temperature.

Morphology, Composition, and Microstructure Characterizations. The morphology and microstructure of the samples were systematically characterized using cold-field scanning electron microscopy (SEM, FEI Quanta 400 FEG) and X-ray diffraction (XRD, D8 Advance, Bruker AXS). Surface chemical properties were examined by X-ray photoelectron spectroscopy (XPS, Axis Ultra DLD, Kratos). Water contact properties were measured by a contact angle (CA) system (OCA 20, Dataphysics Instruments) with 4 μL droplets under an ambient condition.

RESULTS AND DISCUSSION

SEM images (panels a and b of Figure 1) of an as-grown sample show that InGaN nanotips grow vertically on the GaN film with a tip diameter of about 7 nm and a length of around 1.7 μm (see Figures S1 and S2a of the Supporting Information). From the XRD pattern (Figure 1c), the strong peak at 33.4° can be well-indexed as wurzite InGaN (0002), while the peaks at 34.4° and 61.6° originated from wurzite GaN (0002) and Si (100), respectively. The absence of other diffraction peaks reveals that the InGaN nanotips with ⟨0001⟩ orientation grow vertically on ⟨0001⟩ GaN film. The ratio of the indium component was calculated to be 0.34 according to the Vegard law.[22] The photoluminescence (PL) presents a peak at 576 nm with a band gap of 2.15 eV. Well-crystallized InGaN nanotips without phase separation can be seen from selected area electron diffraction (SAED) in Figure S2b of the Supporting Information.

Water CAs of the as-grown InGaN nanotip arrays were measured to be about 96°, as shown in Figure 2a. After Piranha solution treatment, a thin oxide layer was formed on the surface of the InGaN nanotips,[23] showing a superhydrophilic property with a CA of almost 0° (Figure 2b). XPS evidence (see Figure S3 of the Supporting Information) revealed that a significant amount of the hydroxyl group increased on the nanotip surfaces after the oxidation. A capillary effect of the hydroxyl surface of nanostructures was believed to be responsible for superhydrophilic formation on the surface.[24] After the OPA modification, InGaN nanotip arrays had a water CA of 154° (Figure 2c). No changes of CAs were observed when the samples were stored in the dark for 2 months. In contrast, the CAs decreased to 18.6° (Figure 2d) by a UV light illumination for 90 min.

It is reported that trapped air among the nanotips plays a key role in superhydrophobic behavior[2] after polar molecule coating, which can be interpreted by the Cassie−Baxter wetting regime.[25] In our opinion, both surface residue groups and nanostructures played important roles in wetting behaviors of InGaN nanotip arrays.[26] The nanotip arrays took a "point contact" behavior, which produced a discrete three-phase contact line with lesser capillary force.[27] The wetted area fraction of InGaN nanotip arrays can be calculated to be 7.7% using Cassie's equation:[28] $\cos\theta_r = f\cos\theta - (1-f)$, where θ_r and θ represented the water CAs of nanotip arrays and smooth surfaces, respectively, and f was the area fraction of the solid−liquid contact. We can deduce that θ_r increases with an increase of θ or a decrease of f. Moreover, θ and f are determined by the surface residue groups and nanostructures, respectively. OPA modifications can significant increase θ, while nanotip structures can obtain quite a low f. Experiments had been conducted to verify the influence of the above two factors on the wettability of InGaN nanotip arrays. As seen from Table S1 of the Supporting Information, in comparison to InGaN plane samples grown with MOCVD, InGaN nanotip arrays became superhydrophilic without OPA coating and superhydrophobic after OPA coating. Surface residue groups determined whether the surface was hydrophilic or hydrophobic, while the nanostructure morphology can enhance the corresponding wetting behavior. This kind of nanostructure had intrinsic properties of low coefficient viscosities and ice-repellent abilities.[29]

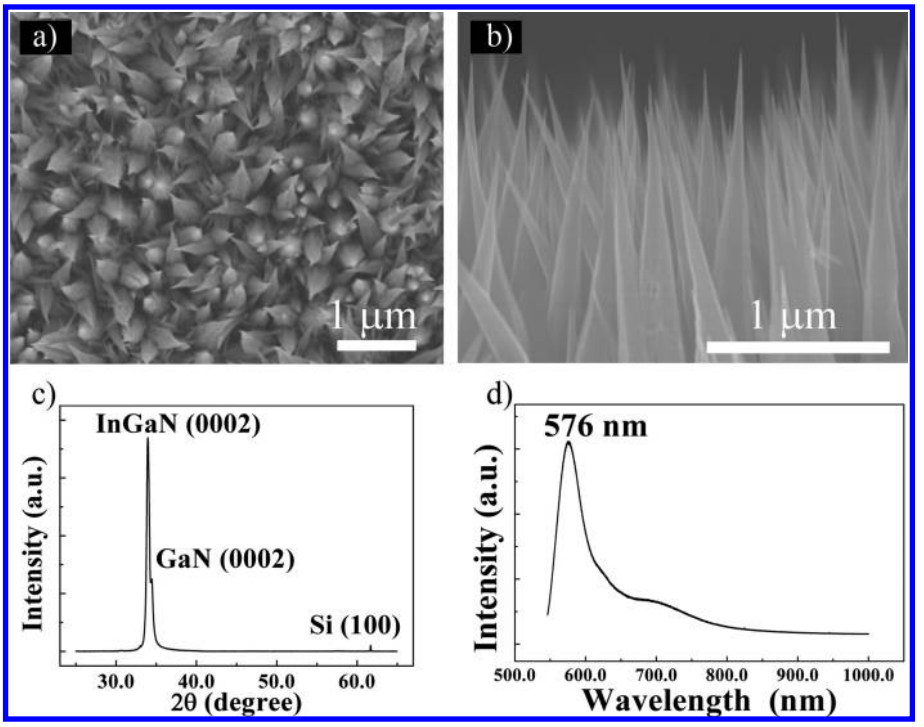

Figure 1. (a) Top view and (b) side view of SEM images, (c) XRD pattern, and (d) room-temperature photoluminescence spectrum for the as-grown sample.

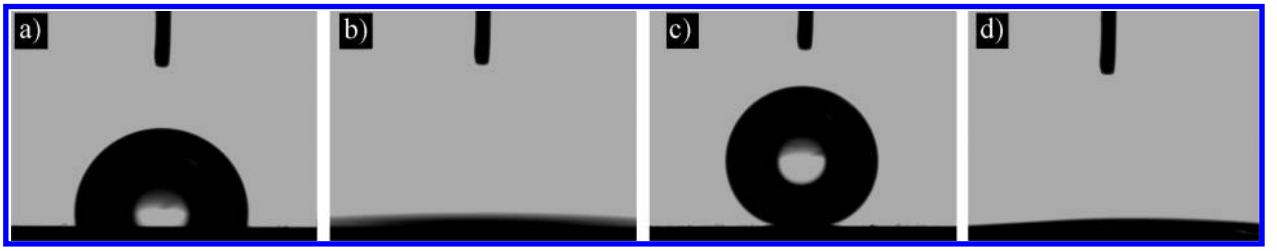

Figure 2. Water CA measurements of the sample (a) pre-oxidation, (b) pre-OPA coating, (c) post-OPA modification, and (d) post-UV irradiation.

After UV treatment, OPA molecules decomposited under the photogenerated active radicals (e.g., •OH) and the InGaN surfaces became back to hydrophilic by a capillary effect.

Light-induced wettability transformation was further examined by measuring CAs as a function of exposure time, as shown in Figure 3a. While UV and visible light illumination time increased from 0 to 90 min, the CAs decreased from 154° to 18.6° and from 155.7° to 76.3°, respectively. The CA of samples under 90 min of visible light is higher than that under 90 min of UV light, which may be caused by both the illuminator with the lower power of the xenon lamp (300 W) than the mercury lamp (400 W) and a power loss because of the 400 nm wavelength high-pass filter. Additionally, the CAs keep decreasing to 43.6° after 160 min of visible light irradiation. These superhydrophobic to hydrophilic changes could be switched by alternating UV exposure and OPA coating (Figure 3b). The slightly increasing CAs after the second round of the UV/OPA process may be caused by insoluble octyl alcohol residuals on the nanotip surface. The hydrophilic surface, which was illuminated with a visible lamp, can also be converted to hydrophobic after grafting OPA again, as shown in Figure S4 of the Supporting Information. Such switching showed a great reproducibility during several repeating experiments because of the excellent chemical stability of InGaN in aqueous solutions.[17b]

To investigate the wettability switching mechanism, XPS was employed to quantify element ratio changes (especially P and C) after the OPA modification (Figure 4a) and UV illumination (full wide spectrum of InGaN after UV treatment in Figure S5 of the Supporting Information). Panels b and c of Figure 4 were P2p and C1s XPS peaks of InGaN before (IG0) and after (IG1) OPA modification and after UV irradiation (IG2) for 50 min, respectively. The P2p peak at 133.2 eV and C1s peak at 284.8 eV were greatly enhanced after the OPA coating because of increasing OPA molecules on the surface. Moreover, those peak intensities decreased dramatically after the UV treatment, implying a significant reduction of OPA molecules on the surface. Element atom ratios were calculated from a relative intensity of the elements, as summarized in Table 1. In comparison to ratios of InGaN nanotip arrays before OPA coating, ratios of phosphorus/indium (P/In) and carbon/indium (C/In) after OPA modification increased from ~0 and 1.535 to 0.695 and 10.96, respectively, which indicated surface grafting of OPA. These results are

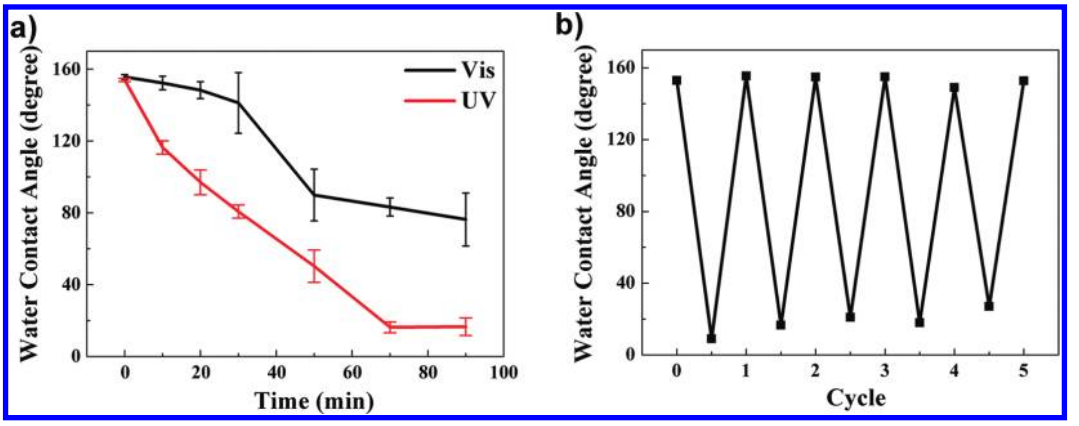

Figure 3. (a) Water CA plots of OPA-modified InGaN nanotip arrays as a function of the illumination time under UV and visible light. (b) Superhydrophobic−hydrophilic transitions of the InGaN nanotip arrays by switching UV treatment and OPA deposition.

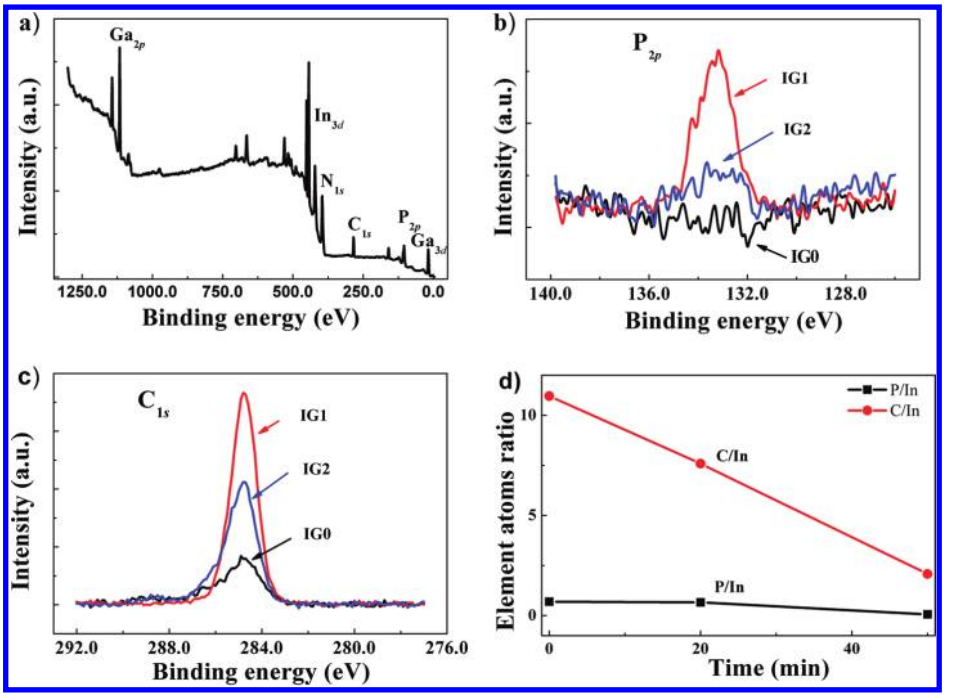

Figure 4. (a) Full wide XPS spectrum of OPA-modified InGaN nanotip arrays. (b) P2p and (c) C1s XPS spectra of the samples pre-OPA coating (IG0), post-OPA coating (IG1), and post-UV illumination (IG2). (d) Ratios of P/In and C/In as a function of the UV illumination time.

consistent with the CA measurements shown in Figure 2. The phosphorus/carbon (P/C) was 0.063 after the OPA grafting, which was in excellent agreement with results from room-temperature micro-Raman measurements.[30]

Considering the band gap of the InGaN nanotip arrays straddles redox potentials of O_2/H_2O and H^+/H_2, the active radicals (e.g., •OH, $•O^{2-}$, and •OOH) can be generated via photogenerated electron−hole pairs in InGaN (see Figure S6 of the Supporting Information).[31] A similar process that took place on TiO_2 with the P−C bond was reported to disappear by forming a $-P-O^-$ residue and carbon oxygen groups.[32] In this process, XPS signals of C1s will dramatically decrease, while no significant reduction of P2p signals can be observed. However, in our experiments, both P2p and C1s signals dropped after UV illumination (panels b and c of Figure 4), indicating a different mechanism.

Table 1. P/In, C/In, and P/C Ratios of InGaN Samples by OPA Coating and Subsequent UV Illumination for 50 min

	OPA coating		
	before	after	UV treatment
P/In	0	0.695	0.059
C/In	1.535	10.96	2.08
P/C	0	0.063	0.028

In comparison to the C1s spectrum before UV illumination, a significant increase of C−O, C═O, and O−C═O groups can be found on the C1s after 90 min of UV exposure (see Figure S7 of the Supporting Information). In contrast, after UV illumination, P/In, C/In, and P/C ratios turned out to be 0.059, 2.08, and

dx.doi.org/10.1021/la203072n |*Langmuir* 2011, 27, 13220–13225

Scheme 2. Schematic Diagrams of OPA Modification and a Bond-Scission Mechanism on InGaN Nanotips by UV−vis Illumination

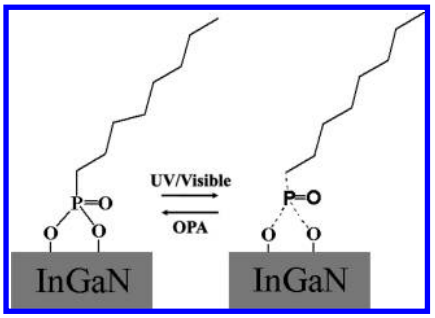

0.028, respectively (in Table 1), which implied that both P−C and MO−P bonds were broken in the photoinduced decomposition process (Scheme 2). The slope of the P/In curve was lower than that of the C/In curve (Figure 4b and data shown in Table 1), which originated from the higher bond dissociation energy of the MO−P bond (589 kJ/mol) than the P−C bond (507 kJ/mol).[33] Considering that pyrophosphate is obtainable only via harsh conditions and will depolymerize in aqueous solutions,[34] reattachment of OPA onto the InGaN nanotip arrays (Figure 3b and Scheme 2) further suggested the bond breaking of MO−P by light illumination. Because of a highly tunable band gap, with small lattice constants and strong bonding energies, InGaN-based devices can work at high-temperature and high-power conditions[35] and stabilize in aqueous solution.[19b,20]

To further address the subsequent effect of UV−vis light on the InGaN nanotips, SEM imaging after UV irradiation was carried out accordingly. No significant surface degradation was observed on the InGaN nanotips, as illustrated in Figure S8 of the Supporting Information, which definitely indicated that the photoinduced decomposition had a dominant effect on the OPA molecules of InGaN nanotip surfaces.

CONCLUSION

A novel fabrication method was demonstrated for hydrophobic Group III−V nanotip arrays. A thin layer of oxide forms on the surface of InGaN nanotip arrays, which facilitate OPA coating. The water CAs significantly decreased after the OPA-grafted samples were exposed to UV−vis light for about 90 min. It is believed that both P−C and MO−P (M = In and Ga) bond breaking under UV−vis illumination induces wettability changes, which was further validated by XPS. Furthermore, no significant surface degradation of the InGaN nanotip arrays was observed after UV−vis irradiation. The studies of superhydrophobic−hydrophilic switching phenomena on InGaN nanotip arrays and the photocatalysis properties have potential applications for the design and optimization of Group III−V materials in solar cells, light-emitting diodes (LEDs), water splitting, actuators, and microfluidic devices.

ASSOCIATED CONTENT

Supporting Information. SEM image of InGaN nanotips at high magnification (Figure S1), TEM micrograph and SAED pattern (Figure S2), water CAs of InGaN wafer and nanotip arrays before and after OPA coating (Table S1), XPS spectra before and after oxidation (Figure S3), wettability transition under visible light (Figure S4), full wide XPS spectrum after UV irradiation (Figure S5), band-gap diagram (Figure S6), C1s XPS spectra (Figure S7), and SEM images after UV treatment (Figure S8). This material is available free of charge via the Internet at http://pubs.acs.org.

AUTHOR INFORMATION

Corresponding Author
*E-mail: gscheng2006@sinano.ac.cn.

ACKNOWLEDGMENT

This work was partially funded by the Key Program of the National Science Foundation of China (Award 10834004) and the China Postdoctoral Science Foundation (20100471393). We are grateful for the professional services of Platforms of Characterization and Test and the Nanofabrication Facility at the Suzhou Institute of Nano-Tech and Nano-Bionics, Chinese Academy of Sciences. We thank Professor Xuefeng Gao for the measurements of water CAs, Dr. Qi Zhang and Dr. Youpin Gong for helpful discussion, and Dr. Beibei Zhang for assisting in XPS measurements.

REFERENCES

(1) Martinez, G. L.; Curiel, M. R.; Skromme, B. J.; Molnar, R. J. *J. Electron. Mater.* **2000**, *29*, 325.
(2) Cassie, A. B. D.; Baxter, S. *Trans. Faraday Soc.* **1944**, *40*, 0546.
(3) (a) Barberoglou, M.; Zorba, V.; Pagozidis, A.; Fotakis, C.; Stratakis, E. *Langmuir* **2010**, *26*, 13007. (b) Garnett, E.; Yang, P. D. *Nano Lett.* **2010**, *10*, 1082.
(4) Li, H. Y.; Jiang, B.; Schaller, R.; Wu, J. F.; Jiao, J. *J. Phys. Chem. C* **2010**, *114*, 11375.
(5) Kwak, G.; Lee, M.; Yong, K. *Langmuir* **2010**, *26*, 9964.
(6) Kim, T. I.; Baek, C. H.; Suh, K. Y.; Seo, S. M.; Lee, H. H. *Small* **2008**, *4*, 182.
(7) Kwak, G.; Lee, M.; Yong, K. *Langmuir* **2010**, *26*, 9964.
(8) (a) Borras, A.; Barranco, A.; Gonzalez-Elipe, A. R. *Langmuir* **2008**, *24*, 8021. (b) Sun, R. D.; Nakajima, A.; Fujishima, A.; Watanabe, T.; Hashimoto, K. *J. Phys. Chem. B* **2001**, *105*, 1984.
(9) Papadopoulou, E. L.; Pagkozidis, A.; Barberoglou, M.; Fotakis, C.; Stratakis, E. *J. Phys. Chem. C* **2010**, *114*, 10249.
(10) Yao, X.; Song, Y.; Jiang, L. *Adv. Mater.* **2011**, *23*, 719.
(11) Kwak, G.; Seol, M.; Tak, Y.; Yong, K. *J. Phys. Chem. C* **2009**, *113*, 12085.
(12) (a) Parkin, I. P.; Palgrave, R. G. *J. Mater. Chem.* **2005**, *15*, 1689. (b) Schmuki, P.; Song, Y. Y.; Roy, P.; Paramasivam, I. *Angew. Chem., Int. Ed.* **2010**, *49*, 351.
(13) Wang, J.; Mao, B.; Gole, J. L.; Burda, C. *Nanoscale* **2010**, *2*, 2257.
(14) Chin, V. W. L.; Tansley, T. L.; Ostochan, T. *J. Appl. Phys.* **1994**, *75*, 7365.
(15) Kida, T.; Minami, Y.; Guan, G.; Nagano, M.; Akiyama, M.; Yoshida, A. *J. Mater. Sci.* **2006**, *41*, 3527.
(16) (a) Fahrenkopf, N. M.; Shahedipour-Sandvik, F.; Tokranova, N.; Bergkvist, M.; Cady, N. C. *J. Biotechnol.* **2010**, *150*, 312. (b) Cimalla, I.; Will, F.; Tonisch, K.; Niebelschutz, M.; Cimalla, V.; Lebedev, V.; Kittler, G.; Himmerlich, M.; Krischok, S.; Schaefer, J. A.; Gebinoga, M.; Schober, A.; Friedrich, T.; Ambacher, O. *Sens. Actuators, B* **2007**, *123*, 740.
(17) (a) Pan, H.; Gu, B.; Eres, G.; Zhang, Z. *J. Chem. Phys.* **2010**, *132*, 104501. (b) Aryal, K.; Pantha, B. N.; Li, J.; Lin, J. Y.; Jiang, H. X. *Appl. Phys. Lett.* **2010**, *96*, 052110.
(18) Wu, J.; Walukiewicz, W.; Yu, K. M.; Ager, J. W.; Haller, E. E.; Lu, H.; Schaff, W. J.; Saito, Y.; Nanishi, Y. *Appl. Phys. Lett.* **2002**, *80*, 3967.

(19) (a) Usui, S.; Kikawa, S.; Kobayashi, N.; Yamamoto, J.; Ban, Y.; Matsumoto, K. *Jpn. J. Appl. Phys.* **2008**, *47*, 8793. (b) Li, J.; Lin, J. Y.; Jiang, H. X. *Appl. Phys. Lett.* **2008**, *93*, 162107.
(20) Jung, H. S.; Hong, Y. J.; Li, Y.; Cho, J.; Kim, Y. J.; Yi, G. C. *ACS Nano* **2008**, *2*, 637.
(21) Nakamura, S.; Senoh, M.; Iwasa, N.; Nagahama, S.; Yamada, T.; Mukai, T. *Jpn. J. Appl. Phys.* **1995**, *34*, 1332.
(22) Denton, A. R.; Ashcroft, N. W. *Phys. Rev. A: At., Mol., Opt. Phys.* **1991**, *43*, 3161.
(23) Douglass, K.; Hunt, S.; Teplyakov, A.; Opila, R. L. *Appl. Surf. Sci.* **2010**, *257*, 1469.
(24) (a) Bico, J.; Thiele, U.; Quere, D. *Colloids Surf., A* **2002**, *206*, 41. (b) Bico, J.; Tordeux, C.; Quere, D. *Europhys. Lett.* **2001**, *55*, 214.
(25) (a) McHale, G. *Langmuir* **2007**, *23*, 8200. (b) Martines, E.; Seunarine, K.; Morgan, H.; Gadegaard, N.; Wilkinson, C. D. W.; Riehle, M. O. *Nano Lett.* **2005**, *5*, 2097.
(26) (a) Jiang, L.; Feng, X. J. *Adv. Mater.* **2006**, *18*, 3063. (b) Lin, C. J.; Lai, Y. K.; Huang, J. Y.; Zhuang, H. F.; Sun, L.; Nguyen, T. *Langmuir* **2008**, *24*, 3867.
(27) Lin, C. J.; Lai, Y. K.; Gao, X. F.; Zhuang, H. F.; Huang, J. Y.; Jiang, L. *Adv. Mater.* **2009**, *21*, 3799.
(28) Quere, D.; Lafuma, A. *Nat. Mater.* **2003**, *2*, 457.
(29) Kulinich, S. A.; Farhadi, S.; Nose, K.; Du, X. W. *Langmuir* **2011**, *27*, 25.
(30) Raman, A.; Dubey, M.; Gouzman, I.; Gawalt, E. S. *Langmuir* **2006**, *22*, 6469.
(31) (a) Moses, P. G.; Van de Walle, C. G. *Appl. Phys. Lett.* **2010**, 96. (b) Mi, Z. T.; Wang, D. F.; Pierre, A.; Kibria, M. G.; Cui, K.; Han, X. G.; Bevan, K. H.; Guo, H.; Paradis, S.; Hakima, A. R. *Nano Lett.* **2011**, *11*, 2353.
(32) (a) Balaur, E.; Macak, J. M.; Taveira, L.; Schmuki, P. *Electrochem. Commun.* **2005**, *7*, 1066. (b) Minabe, T.; Tryk, D. A.; Sawunyama, P.; Kikuchi, Y.; Hashimoto, K.; Fujishima, A. *J. Photochem. Photobiol., A* **2000**, *137*, 53. (c) Lee, J. P.; Kim, H. K.; Park, C. R.; Park, G.; Kwak, H. T.; Koo, S. M.; Sung, M. M. *J. Phys. Chem. B* **2003**, *107*, 8997.
(33) In *CRC Handbook of Chemistry and Physics*, 87th ed.; Lide, D. R., Ed.; CRC Press (Taylor and Francis Group): Boca Raton, FL, 2006; p 9.
(34) Malowan, J. E. *Inorg. Synth.* **1950**, *3*, 96.
(35) Pearton, S. J.; Kang, B. S.; Kim, S. K.; Ren, F.; Gila, B. P.; Abernathy, C. R.; Lin, J. S.; Chu, S. N. G. *J. Phys.: Condens. Matter* **2004**, *16*, R961.